American Journal of Pathology, Vol. 164, No. 3, March 2004

Animal Model

Morpho-Regulation of Ectodermal Organs

Integument Pathology and Phenotypic Variations in K14-Noggin Engineered Mice through Modulation of Bone Morphogenic Protein Pathway

Maksim Plikus,* Wen Pin Wang,*† Jian Liu,* Xia Wang,* Ting-Xin Jiang,* and Cheng-Ming Chuong*

From the Department of Pathology, Keck School of Medicine, University of Southern California, Los Angeles, California; and the Graduate Institute of Molecular and Cellular Biology,† Tzu Chi University, Hualien, Taiwan*

Ectodermal organs are composed of keratinocytes organized in different ways during induction, morphogenesis, differentiation, and regenerative stages. We hypothesize that an imbalance of fundamental signaling pathways should affect multiple ectodermal organs in a spatio-temporal-dependent manner. We produced a K14-Noggin transgenic mouse to modulate bone morphogenic protein (BMP) activity and test the extent of this hypothesis. We observed thickened skin epidermis, increased hair density, altered hair types, faster anagen re-entry, and formation of compound vibrissa follicles. The eyelid opening was smaller and ectopic cilia formed at the expense of Meibomian glands. In the distal limb, there were agenesis and hyperpigmentation of claws, interdigital webbing, reduced footpads, and *trans*-differentiation of sweat glands into hairs. The size of external genitalia increased in both sexes, but they remained fertile. We conclude that modulation of BMP activity can affect the number of ectodermal organs by acting during induction stages, influence the size and shape by acting during morphogenesis stages, change phenotypes by acting during differentiation stages, and facilitate new growth by acting during regeneration stages. Therefore during organogenesis, BMP antagonists can produce a spectrum of phenotypes in a stage-dependent manner by adjusting the level of BMP activity. The distinction between phenotypic variations and pathological changes is discussed. *(Am J Pathol 2004, 164:1099–1114)*

The integument forms the interface between an organism and its environment. During development and evolution, different types of epithelial organs form on the body surface to allow animals to adapt to different environments. Although these organs, such as hairs, glands, teeth, and so forth, appear to be very different in structure and function, developmental studies suggested that they are all products of epithelial-mesenchymal interactions, with variations overlaid on a common theme.[1] Genes involved in human ectodermal dysplasias have recently been cloned. These studies show that a single gene defect can cause abnormalities in several ectodermal organs.[2–4] This further substantiates the notion that fundamental molecular pathways are frequently shared in the building of different epithelial organs. The commonly used molecular pathways include bone morphogenic protein (BMP), fibroblast growth factor (FGF), sonic hedgehog (SHH), Wnt, Notch, Eda pathways and so forth.[5,6] In each pathway there are multiple ligands, receptors, intracellular signaling transducers, and extracellular antagonists. Knowledge of these pathways motivates us to investigate how these molecular activities are translated into tissue morphogenesis. In the context of tissue engineering, such knowledge will also be required to guide epithelial stem cells appropriately to form the tissues/organs desired.

Here we selected the BMP pathway for further analysis.[7] BMPs play an important role in many developmental

Supported by the National Institute of Arthritis and Musculoskeletal and Skin Diseases (AR42177 and AR47364 to C.M.C.); Tzu-Chi University (to W.P.W.); and the National Institutes of Health (grant NIH 1 P03 DK48522 to The Microscopy Sub Core at the University of Southern California Center for Liver Diseases).

M.P. and W.P.W. contributed equally to this study.

Accepted for publication November 14, 2003.

Address reprint requests to Cheng-Ming Chuong, M.D., Ph.D., Department of Pathology, University of Southern California, HMR 315B, 2011 Zonal Ave., Los Angeles, CA 90033. E-mail: chuong@pathfinder.usc.edu.

systems. Initially identified for their effects on osteocyte proliferation and differentiation, BMPs were further shown to act as regulators of proliferation, differentiation, apoptosis, cell adhesion, and migration during the development of multiple organs in many organisms studied.[8–10] Loss-of-function mutations of various components of the BMP pathway lead to severe developmental abnormalities often resulting in early embryonic lethality.[11] The effect of BMPs on proliferation, differentiation, and apoptosis in different developmental systems is complex. It is, however, concentration-dependent. Low or high dosages of BMPs often result in opposite cell fate decisions: either proliferation or apoptosis.[12] BMP activity in a given tissue depends on the concentration and distribution of BMPs and their antagonists. A number of secreted proteins including Noggin, Follistatin, Chordin, and others antagonize BMP-mediated signaling.[13] Noggin is the most powerful BMP-2 and BMP-4 antagonist.[14,15] Different effects of BMPs are often mediated by distinct BMP receptors (BMPRs). Several models suggest that the proliferative effect of BMPs is mainly mediated via BMP receptor IA (BMPR-IA).[16,17] Apoptotic signaling is mainly mediated through the receptor BMPR-IB.[18,19]

BMP signaling is used in skin and skin appendages development. In the presence of BMP-4, ectodermal cells choose an epidermal over a neural fate early in gastrulation.[20] Later in skin development, distinct spatial distributions of different BMPs and BMPRs are seen. BMP-6 and BMP-7 are mainly expressed in the epidermis, with BMP-7 present in the basal and BMP-6 in suprabasal layers.[21–23] Also, BMPR-IA is expressed in the basal layer, whereas BMPR-IB is in the suprabasal layer. Based on several lines of evidence it was proposed that BMPR-IA mediates proliferation effects and BMPR-IB mediates differentiation effects of BMPs in epidermis.[17] Unlike BMP-6 and BMP-7, BMP-2 and BMP-4 are expressed during hair follicle (HF) organogenesis. BMP-4 is expressed transiently in the mesenchymal condensations just before HF formation. Therefore, this may be part of the initial dermal signals inducing follicular germ formation. BMP-2, however, is expressed in the epidermal placode, and in more advanced follicles it is found in the matrix and precortex cells.[21,24,25] At the time of HF induction, BMP signaling inhibits induction whereas Noggin signaling stimulates induction of HFs.[25,26] Importantly, induction of secondary (nontylotrich) HFs, but not primary (tylotrich) HFs is affected by BMPs/Noggin.[27]

The role of Noggin during HF induction was addressed in the Noggin knockout mouse model.[25] Data were provided using Noggin knockout skin grafts because homozygous Noggin knockout mice die prematurely. It suggests that Noggin is important for secondary HF induction. In this model, secondary HFs failed to form. Induction of primary HFs was not affected, yet their growth was further arrested because of long-term BMP excess. Similar to this, transgenic mice engineered to overexpress BMP-4 in the outer root sheath under the control of the bovine cytokeratin IV promoter had a complete deficiency of hair growth after the first hair cycle and, therefore, were progressively balding.[28] It seems that during development, Noggin prevents interactions between BMPR-IA and BMPs produced by the mesenchyme and placode. In support of this idea, Noggin treatment increases the hair placodes and accelerates HF morphogenesis in embryonic skin organ culture.[25] Noggin is also required for HF growth during postnatal life. Normally, in adult HFs, Noggin activity is localized to the HF bulb. Noggin, produced by the dermal papilla, supports proliferation in the lower hair matrix.[25] Overexpression of Noggin in proliferating hair matrix cells and differentiating hair precursor cells under the proximal Mxs2 promoter leads to the disruption of differentiation in epithelial cells controlled here, in part, by BMPs.[29] Another important pathway in hair morphogenesis is Wnt/β-catenin signaling and its up-regulation leads to an induction of excessive numbers of HFs.[30,31] Disruption of the Wnt/β-catenin pathway in skin leads to an arrest of HF development.[32,33] Inhibition of BMP activity is shown to produce Lef-1 required for the activation of β-catenin/Lef-1 transcriptional complex.[25,34]

Although the roles of Noggin in HF formation have been studied, its role in other skin appendages remains mostly unknown. To address these questions we created a transgenic mouse model in which ectopic Noggin expression was directed by the K14 promoter. The K14-Noggin mice study showed that Noggin mediates disruption of normal BMP signaling during development, causing multiple abnormalities in a variety of ectodermal organs. Hyperplasia of pelage HFs occurred, ectopic HFs formed on the ventral side of the paw, supernumerary cilia formed in eyelids, and compound vibrissa follicles arose. Claws and footpads failed to form normally. There were also defects in organs that we do not normally consider as skin appendages. For example, we found an increase in the sizes of external genitalia and defects in eyelid opening. Here, we will describe an array of abnormalities and discuss the roles of BMP activity in pathogenesis.

Materials and Methods

Production and Genotyping of Transgenic Mice

Mice were generated in the Norris Cancer Center transgenic mouse facility at the University of Southern California. To generate transgenic mice, human K14 promoter-chicken *Noggin*-poly A inserts were purified and microinjected into the male pronucleus of fertilized egg of C57BL/6J × CBA/J mice followed by reimplantation of injected eggs into pseudopregnant C57BL/6J × CBA/J females. The purification and microinjection of DNA were performed as described.[36] The founder K14-Noggin mice were then backcrossed onto C57BL/6J background for six generations. All phenotypical features of K14-Noggin mice showed high penetrance.

Mice were screened for transgene presence by polymerase chain reaction (PCR) using chicken Noggin construct-specific primers: 5′-CCAGATCTATGGATCATTCCCAGTGC-3′ and 5′-GGAGATCTCTAGCAGGAGCACTTGCA-3′. Tail genomic DNA was extracted as described in manufacturer's protocol (Qiagen, Valencia,

CA). PCR products were amplified in separate reactions using the three-stage PCR program: 94°C for 2 minutes; 94°C for 1 minute, 55°C for 1 minute, 72°C for 1 minute (30 cycles); 72°C for 10 minutes. The identities of the founder mice were confirmed by Southern blot analyses.

Quantitative Genotyping

Quantitative genotyping of K14-Noggin mice was done by real-time quantitative PCR using SYBR Green technology.[37] The reaction and detection were performed in GeneAmp 5700 (see the User Manual; PE Applied Biosystems, Foster City, CA). A separate set of primers was designed for chicken Noggin to be used for real-time quantitative PCR: 5′-TCTGTCCCAGAAGGCATGGT-3′ and 5′-CGCCACCTCAGGATCGTTAA-3′. To control differences in the quantity of DNA template, the mouse L-32 gene was amplified in parallel for each sample and was used as a normalization factor to calculate the relative amount of chicken Noggin in mouse genomic DNA. The following L-32-specific primers were used: 5′-TGGTTTTCTTGTTGCTCCCATA-3′ and 5′-GGGTGCGGAGAAGGTTCAA-3′. A detailed protocol for real-time quantitative PCR is described elsewhere.[38]

Among all K14-Noggin mice tested, we selected one mouse that showed the highest dC_T value (5.5) on real-time quantitative PCR (C_T, cycle threshold value; $dC_T = C_T$ of Noggin $- C_T$ of L-32 for the same sample). This mouse contained the lowest number of K14-Noggin in the genome. Relative amount of K14-Noggin in all other mice was calculated as following: fold difference $= 2 \times (5.5 - dC_T)$.

Quantitative Reverse Transcriptase (RT)-PCR

The amount of chicken Noggin mRNA in K14-Noggin mice tissue was measured using the real-time quantitative RT-PCR method, based on SYBR Green technology, mentioned above. RNA was extracted from the ear pinna using the RNeasy mini kit, following the manufacturer's protocol (Qiagen). Ear pinna was selected for this experiment because it contains two layers of K14-expressing epidermis within relatively small amount of tissue. Real-time PCR was performed using identical set of primers and following the same protocol as for the quantitative genotyping described above. Relative amount of Noggin mRNA in mice tissue was calculated as following: fold difference $= 2 \times (9.45 - dC_T)$, where 9.45 is the dC_T value for the mouse with the lowest level of chicken Noggin mRNA in the tested tissue.

Histological, Histochemical, and Immunohistological Staining

Tissues were collected and fixed in 4% paraformaldehyde in phosphate-buffered saline (PBS), dehydrated, embedded in paraffin, and sectioned at 5 to 6 μm. When necessary, specimens were additionally decalcified in Immunocal solution (American Mastertech Scientific, Lodi, CA) for 48 hours at 4°C after fixation. Standard hematoxylin and eosin (H&E) staining was performed for basic histological analysis.

Frozen tissue sections were used for the tyramide-based tyrosinase assay.[39] Briefly, after 3% peroxide treatment, 5% bovine serum albumin (fraction V) and avidin/biotin were used to block nonspecific binding (Vector Laboratories, Burlingame, CA). Next, biotin-tyramide in 1× application diluent (Perkin-Elmer Life Sciences, Emeryville, CA) was applied. After a washing step, streptavidin-CY3 (1:600; Sigma Chemical Co., St. Louis, MO) was applied.

Immunostaining was performed using the Ventana Discovery automated immunostaining module (Ventana Medical Systems, Tucson, AZ). The primary antibodies used were mouse monoclonal anti-proliferating cell nuclear antigen (PCNA) (1:500; Chemicon, Temecula, CA), rabbit anti-K14 (1:400; Berkeley Antibody Company, Richmond, CA), and anti-K10 (1:200, Sigma). The DAB detection kit (Ventana Medical Systems) was used for color development.

In Situ *Hybridization*

Mouse tissues from various ages were used for section in *in situ* hybridization. Section *in situ* samples were fixed and dehydrated according to the standard protocol. All solutions used for the procedure were diethyl pyrocarbonate-treated to inactivate RNase. To detect the RNA expression, the tissue was hybridized with digoxigenin-labeled probes. The signals were detected by using an anti-digoxigenin antibody coupled to alkaline phosphatase. Some samples were processed using the Discovery automated *in situ* hybridization instrument (Ventana Medical Systems).

Whole mount *in situ* procedure was performed on E15 mouse embryos. Specimens were fixed in 4% paraformaldehyde in diethyl pyrocarbonate-treated PBS. Tissue samples were then dehydrated in a series of methanol in PBS and 0.1% Tween 20 (PBT buffer) and stored in absolute methanol at −20°C before the actual staining procedure. Whole mount *in situ* hybridization procedures were performed using the InsituPro automated *in situ* detection module (Intavis AG, Koeln, Germany). Analysis was performed according to the standard whole mount *in situ* protocol.[40]

Morphometric Analysis

All surgical procedures were performed on anesthetized mice (ketamine HCl:xylazine mixture was used). For the whole mount skin preparation, anagen skin was collected, inverted, and subcutaneous tissue was removed. These samples were fixed and dehydrated in a stretched condition. After dehydration, skin samples were cleared with xylene and photographed. Morphometric analyses were then performed using Adobe PhotoShop.

Analysis of hair shaft structure was performed under the inverted microscope according to a previously described protocol.[41,42] The relative number of guard, awl, auchene, and zigzag hairs was determined from the fur of

the dorsal skin. Lengths of the hair growth cycle stages were based on the change of the skin color from pink during telogen to black during anagen. These changes occur because of the active melanogenesis in the HFs during anagen and were proven to be valid criteria for the hair cycle staging elsewhere.[43] All observations were performed on shaved mice ($n = 6$). Several consecutive hair growth cycles were analyzed on the same mice for 4 months. We started when they were 2 months old and ended when they were 6 month old. The lengths of the anagen and telogen stages of the hair growth cycle were established. External genital measurements were performed on anesthetized animals. Nonerect genitalia were measured in both control and K14-Noggin animals.

Scanning Electron Microscopy Analysis

Tissues were prepared according to the standard scanning electron microscopy protocol. Briefly, it includes fixation in 2.5% glutaraldehyde in 0.1 mol/L sodium cacodylate, dehydration, and critical point drying from ethanol. Next, samples were coated with gold in a sputter coat chamber. They were examined by scanning electron microscopy in the Doheny Eye Institute Core Facility, University of Southern California.

Results

Production, Genotyping, and Phenotyping of K14-Noggin Mice

The chicken Noggin cDNA fragment was subcloned into the human K14 vector (Figure 1A).[44] K14-Noggin-PolyA inserts were released from plasmids and used for injection. Three independent transgenic lines were produced with similar phenotypes. Identities of K14-Noggin mice were confirmed by PCR-genotyping using chicken Noggin-specific primers (Figure 1B). We have isolated several lines and found a range of phenotypes. There were mice with severe phenotypic changes (Figure 1C) and mice with moderate alterations. The more severe phenotypes included absence of claws, interdigital webbing of the paws, hypertrichosis all over the body, shortening of the telogen period of the hair growth cycle, and increased size of the genitalia. In other mice pathological changes were milder. We performed quantitative genotyping of the K14-Noggin mice and quantitative RT-PCR for the Noggin mRNA to establish whether strength of phenotypic changes correlates with K14-Noggin transgene copy number in the mouse genome and Noggin expression level. We studied several key phenotypic features of the limbs of every mouse and correlated them with the fold difference values (see Materials and Methods). Based on this we divided all K14-Noggin mice into low-transgenic (TG) copy number and high-TG copy number with fold difference value for high-TG copy number animals equal to 3 and higher (Table 1).

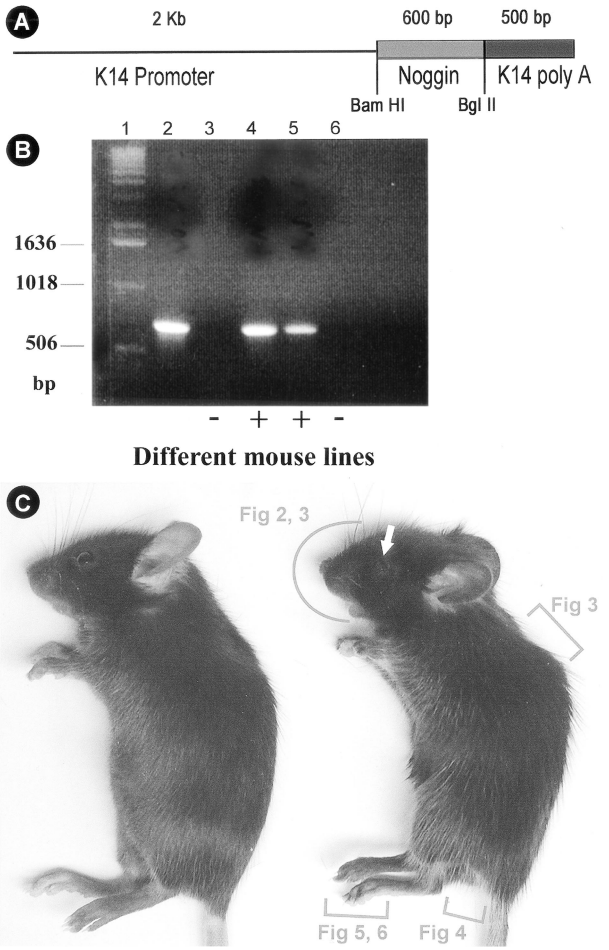

Figure 1. Production of K14-Noggin mouse. **A:** K14 Noggin construct used to generate transgenic mouse. The size of insert used and restriction enzyme are indicated. **B:** Genotyping of K14-Noggin mutant mouse. Products of PCR reaction using specific primers (see Materials and Methods for primers used). **Lane 1**, DNA standard; **lane 2**, positive control—K14-Noggin founder mouse; **lanes 3** and **6**, wild-type mice; **lanes 4** and **5**, K14-Noggin-positive mice. **C:** Appearance of control C57BL/6J (**left**) and mutant K14-Noggin 2.5-month-old mice. Note the obvious hypertrichosis of the K14-Noggin mouse. The eye opening is small (**white arrow**). Digits are not distinctly separated from each other. Regions to be studied further in each figure are marked by **red brackets**.

Phenotypes in the Head

Eyelids

Adult high-TG copy number K14-Noggin mice had smaller eye openings (Figure 2, A and B), whereas the diameters of the eyeballs were not significantly different (3.9 ± 0.5 mm in control mice and 3.75 ± 0.05 mm in high-TG copy number K14-Noggin mice, $n = 3$). Smaller eyelid openings were already obvious as early as postnatal day 14. However, no significant delay of eyelid opening was seen in K14-Noggin mice in comparison with the control mice. In addition, adult eyelids of high-TG copy number K14-Noggin mice exhibited abnormalities. Most significantly, there was formation of ectopic pilosebaceous units at the expense of Meibomian glands. Extra cilia grew in different directions, often pointing inwards

Table 1. Phenotypic Changes in Low- and High-TG Copy Number in K14-Noggin Mice

	High-TG copy number mice (n = 8)*	Low-TG copy number mice (n = 6)*
Genotyping	4.2 ± 0.6†	1
Noggin transcript level	2.9 ± 0.7†	1
Percentage showing phenotype		
Fusion of forelimb digits	100%	12.5 – 25%
Fusion of hindlimb digits	80 –100%	0 – 25%
Absence of forelimb claws	95 –100%	29 – 75%
Absence of hindlimb claws	63 –100%	33 – 58%
Hyperpigmentation of forelimb claws	100%	0 – 60%
Hyperpigmentation of hindlimb claws	70 –100%	40 – 66%

*Number of animals studied.
†Fold difference, calculated as described in Materials and Methods.

toward the cornea, resulting in entropion [Figure 2; B (inset) and G and H (arrows point at inward-growing cilia)]. No prominent corneal lesions were noticed.

We examined the eyelids of newborn mice. Immunohistochemically K14 protein expression was detected in the outer epidermis, conjunctival epithelium, and eye suture of both upper and lower eyelids (Figure 2C). The observed suture defects are consistent with the observation that BMPs are expressed in the eye suture of control E15 mouse embryos. Both BMP4 and BMP2 are expressed in the eye suture epithelium with BMP2 specifically at the conjunctival side and BMP4 throughout the length of the epithelial suture (Figure 2, D and E; these are thick preparations with whole mount *in situ* hybridiza-

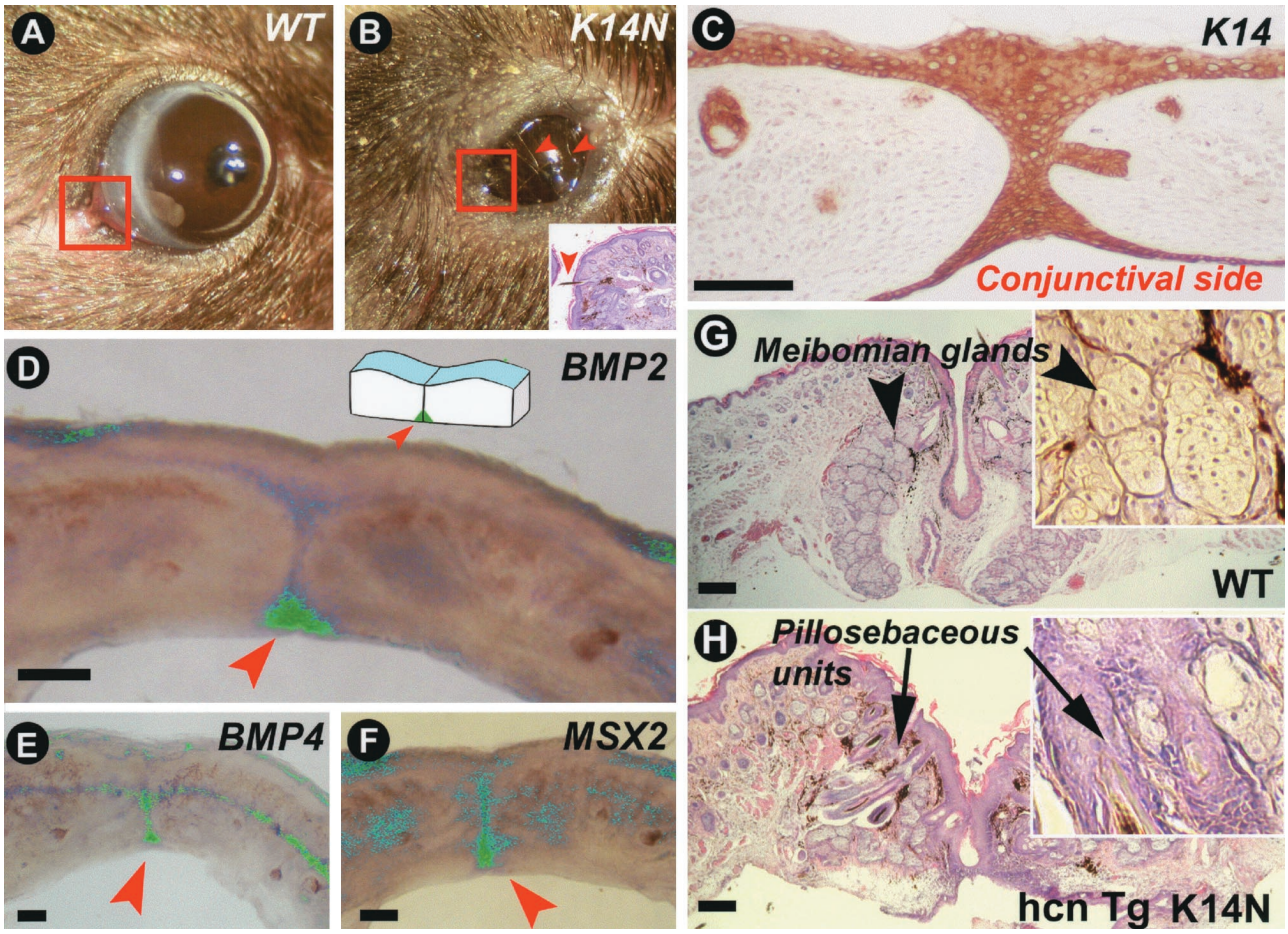

Figure 2. Pathology in eyelid, an epithelial appendage to protect the eye. **A:** Normal size eye slits of 4-month-old control C57BL/6J mouse. **B:** Narrow eye slits in 4-month-old K14-Noggin mouse. Eyelids remain partially fused. Eyeballs are of the same size (not shown). **Arrowheads** point at inward-growing cilia. **C–F:** Eyelid suture of newborn control mouse. **C:** Strong K14 immunostaining is seen in the epidermal side, suture, and conjunctival side of the eyelid. **D–F:** Whole mount *in situ* hybridization of 1-mm-thick eyelid stripe. Green color is computer pseudo-coloring. BMP2 transcripts are expressed predominantly on the conjunctivae side whereas BMP4 is distributed more evenly throughout the eyelid suture. Msx2 transcript distribution is similar to BMP4. **G** and **H:** Corner of eyelids (commissure, corresponding to the areas outlined with red on **A** and **B**) of adult mice. Formation of ectopic pillosebaceous units at the expense of Meibomian glands in high copy number TG K14-Noggin mice (hcn TG K14-Noggin mice). Scale bars, 100 μm.

tion). Msx2 (downstream of BMPs in other systems) is also expressed in the eye suture (Figure 2F).

Vibrissae

Vibrissae are specialized, highly innervated HFs with somatosensory function. Normal mice have one vibrissa emerging from one individual vibrissae follicle, which is enclosed in a collagen capsule (Figure 3, A and C). In high-TG copy number K14-Noggin mice, examination showed that several vibrissae emerged from one orifice (Figure 3B). Histological sections showed that two or three combined vibrissae follicles shared one capsule (Figure 3, D and E). Histological sections showed these compound follicles share a common upper part of the outer root sheath, but have separate lower follicle regions with independent dermal papilla and matrix. They produce separate inner root sheath and vibrissa fibers that open into the same canal. Because they seem to derive from the shared outer root sheath, we consider them to belong to the category of compound HFs.[45]

Phenotypes on the Trunk

Pelage Hair

On the whole body, K14-Noggin mice exhibited a prominent hypertrichosis. The hypertrichosis observed here is a combined result of increased hair density and an excessive mass of hair filaments. Whole mount morphometric analysis of anagen skin from control and K14-Noggin mice was done to quantify hair density and size distribution of HFs (Figure 3, F and G). The wild-type mice hair density was 35.1 ± 2.5 HFs per mm^2. In the high-TG copy number K14-Noggin mice hair density was 63.4 ± 3.9 HFs per mm^2, ~80% higher than the control mouse (Figure 3H). The low-TG copy number K14-Noggin mice hair density was 50.0 ± 7.3 HFs per mm^2, ~42% higher than the control mouse.

The maximal width of the follicles was then measured as an indication of follicle size (Figure 3F, inset, red arrows). In the control mice, all HFs are clearly distributed into two distinct groups: smaller size HFs (secondary HFs) and larger size HFs (primary, guard HFs). In contrast, in high-TG copy number K14-Noggin mice there was no clear fractionationing of the HF sizes (Figure 3I). The majority of HFs were of smaller size, probably representing secondary follicles. Analysis of hair shaft structure showed that high-TG copy number K14-Noggin mice fur contains all four types of hair fibers: guard, awl, auchene, and zigzag. However, high-TG copy number K14-Noggin mice have more awl and auchene hairs than wild-type mice. Our control mice showed 64.3 ± 6% of zigzag hairs and only 27.9 ± 3.6% of awl and auchene hairs, high-TG copy number K14-Noggin mice have 51 ± 4.5% of zigzag and 43.4 ± 3.8% of awl and auchene hairs. We believe that the excessive number of awl and auchene hairs is mostly responsible for the increase in hair density in K14-Noggin mice. Awl and auchene hairs are generally larger than zigzag hairs and this may result in the larger proportion of intermediate sizes of HFs (Figure 3I). Guard hairs are present and appear to have no significant change in their number in K14-Noggin mice.

On the sections of the dorsal trunk skin, control skin contained primary and secondary HFs (Figure 3J). In the K14-Noggin mouse, there were regions of skin with secondary HFs appearing to be normal (not shown) and regions of skin with abnormally enlarged HFs (Figure 3K). There are hypertrophic sebaceous glands and randomly oriented hair fibers. The epidermis of interfollicular skin is thickened. On the sections of the tail, the control skin exhibited secondary HFs and tail scales arranged in a regular pattern (Figure 3L). In the K14-Noggin tail, some regions were relatively normal (not shown) but some regions showed drastic pathology: cystrophic HFs of different sizes pointing to different directions (Figure 3M). Some follicles appeared to have multiple dermal papillae. The density of HFs increased. The dermal layer appears to thicken at the expense of the adipose layer. Whether this is a direct or indirect systematic effect remains to be determined.

Hair Cycle

We measured the length of the anagen and telogen of the hair growth cycle in high-TG copy number K14-Noggin mice. On average, their anagen length was 12.3 ± 1 day, and telogen length was 7.6 ± 2 days. In control mice the anagen length was not significantly different (13.4 ± 1 day), but the telogen length was significantly greater, ranging from 12 to 40 days.

External Genitalia

Compared to wild-type mice, K14-Noggin mice showed distinct differences in their external genitalia. Overall, the sizes of both male and female external genitalia were bigger than those in the control animals (Figure 4; A to D). When freed from the prepuce, the distal segment of the os penis in the K14-Noggin male mice was significantly longer than that of the control mice (Figure 4, F and G). During embryonic development at E15, the tip of growing glans penis expressed high levels of BMP4 (Figure 4E).

Histologically, the preputial lamella was significantly thickened in the K14-Noggin mice. At the same time, the differentiation of hairy spines, mechano-sensory structures of the preputial lamellae, was suppressed. Hairy spines are periodically arranged skin appendages composed of both epidermal and dermal components. They start to differentiate at postnatal week 1 and undergo keratinization at week 2 (Figure 4H). However, in 2-week-old high-TG copy number K14-Noggin mice, hairy spines remained primarily undifferentiated (Figure 4I). *In situ* hybridization showed high levels of BMP4 expression in the epithelial compartment of all hairy spines (Figure 4J). Immunostaining showed strong K14 keratin expression in the basal layers of both the penis and prepuce in the control and K14-Noggin mice (Figure 4, K and L). K10 keratin expression showed that differentiation of hairy

spines in 2-week-old K14-Noggin mice was suppressed (Figure 4, M and N). These mice were fertile.

Phenotypes in the Distal Limb Region

Claw

During embryonic development at E15, BMP4 is specifically expressed in the mesenchyme at the tips of the digits—the sites of claw formation (Figure 5A). K14 keratin is highly expressed in the claw matrix (Figure 5B) and overexpression of Noggin in these regions could potentially perturb claw development. Indeed, a prominent feature of K14-Noggin mice was the claw phenotype. It ranged from split claws in low-TG copy number mice to complete absence in high-TG copy number mice (Figure 5; E to H). Absence of claws in high-TG copy number K14-Noggin mice was coupled with polydactyly and interdigital webbing (Figure 6B).[46]

In the wild-type claw, highly proliferative epithelial cells are confined to one region, known as the claw matrix (Figure 5C). In the low-TG copy number K14-Noggin mice, the claw matrix was not distinct and PCNA-positive cells were not confined to one place, but rather distributed widely in the whole claw region (Figure 5D). This can account for the multiple growth centers and multiple keratinized plates within one claw. Claw plates apparently grew parallel and were separated from each other. Patches of epidermis often separated one plate from another (Figure 5G). In high-TG copy number mutant mice, all claws on forelimbs and almost all claws on hindlimbs were replaced with a thickened cornifying epidermis (Figure 5, H and J).

In control mice, the epidermal differentiation marker K10 keratin is found only in the hyponichium and nail fold, but not in the claw itself (not shown). In the high-TG copy number mutants, the epidermal thickening expressed K10 keratin (Figure 5I). Claws of the low-TG copy number K14-Noggin mice differentiated properly and were K10-negative. Patches of epidermis that separated multiple claw plates from each other were otherwise K10-positive (Figure 5J).

Another interesting phenotype was the pigmentation of the claw. Control mice have black fur, but lack pigmented claws (Figure 5E, inset). In our K14-Noggin mice, we have not seen changes in fur color. However many claws of low-TG copy number K14-Noggin mice and all hindlimb claws of high-TG copy number mutants were hyper-

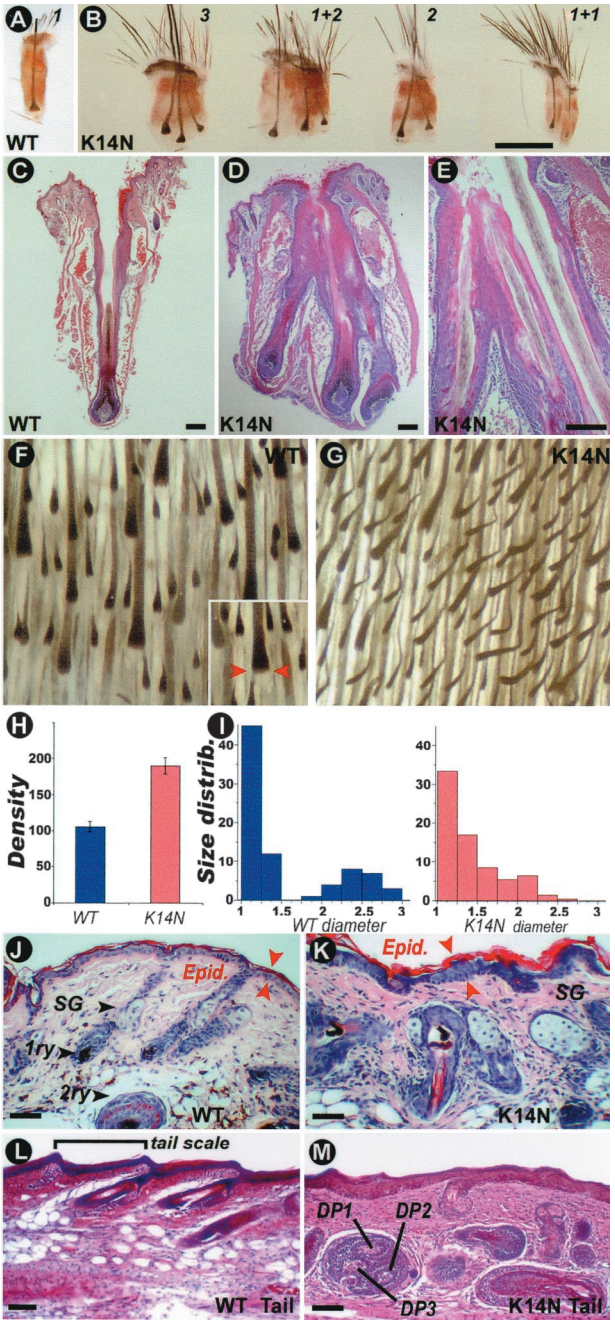

Figure 3. Pathology in vibrissae and pelage hairs. **A** and **B:** Control and K14-Noggin vibrissae HFs. K14-Noggin mice have compound follicles that share one orifice and one capsule. The number in **B** indicates the number of vibrissa filaments that share the same orifice. For example, 1 + 2 means one normal follicle with one filament from one orifice plus one compound follicle with two filaments growing from one orifice. **C–E:** H&E stain of control (**C**) and K14-Noggin (**D**, **E**) vibrissae HFs. K14-Noggin follicles share part of the same outer root sheath, open into the same canal but have a distinct dermal papillae and matrix, and produce a separate inner root sheath and fiber. **F** and **G:** View of inverted skin from the dorsal trunk region of the control and K14-Noggin mice. In the control mouse, all HFs are in anagen. Distinct primary (big) and secondary (small) HFs can be identified. In the K14-Noggin mouse, the density of HFs is increased and the difference between primary and secondary follicles is not obvious. **H:** Density of HFs per 3 mm^2 in control (blue) and K14-Noggin (red) mice. Density is increased by ~80% in the K14-Noggin mouse in comparison with the control mouse. **I:** Relative size distribution of HFs in control (blue) and K14-Noggin (red) mice (size corresponds to the diameter of the hair bulb; see inset in Figure 4F). In the control mouse, HFs clearly fractionate into two distinct groups: those with smaller size (primarily secondary HFs) and those with larger size (primary HFs). In the K14-Noggin mouse, there is no clear fractionation of HFs. The majority of HFs are of intermediate size. This could be because of increased proportion of secondary awl and auchene hairs (see Results). **J** and **K:** H&E staining of skin sections from the back of the control and K14-Noggin 2-week-old mice. Normal secondary and primary (**bottom**) HFs are seen in the control mouse. In some regions of the K14-Noggin mouse, there are enlarged HFs and hypertrophic sebaceous glands. Some hair fibers point to wrong directions. Spacing between follicles is reduced. Skin epidermis is thickened. **L** and **M:** H&E staining of longitudinal sections of the tail from the control and K14-Noggin mice. Different sizes of hypertrophic HFs pointing in different directions are seen in the K14-Noggin mouse. The total number of follicles has increased. Some follicles are dystrophic and appear to have multiple dermal papillae. The epidermal and dermal layers appear thicker. Scale bars: 1 mm (**B**); 100 μm (**C–E** and **J–M**).

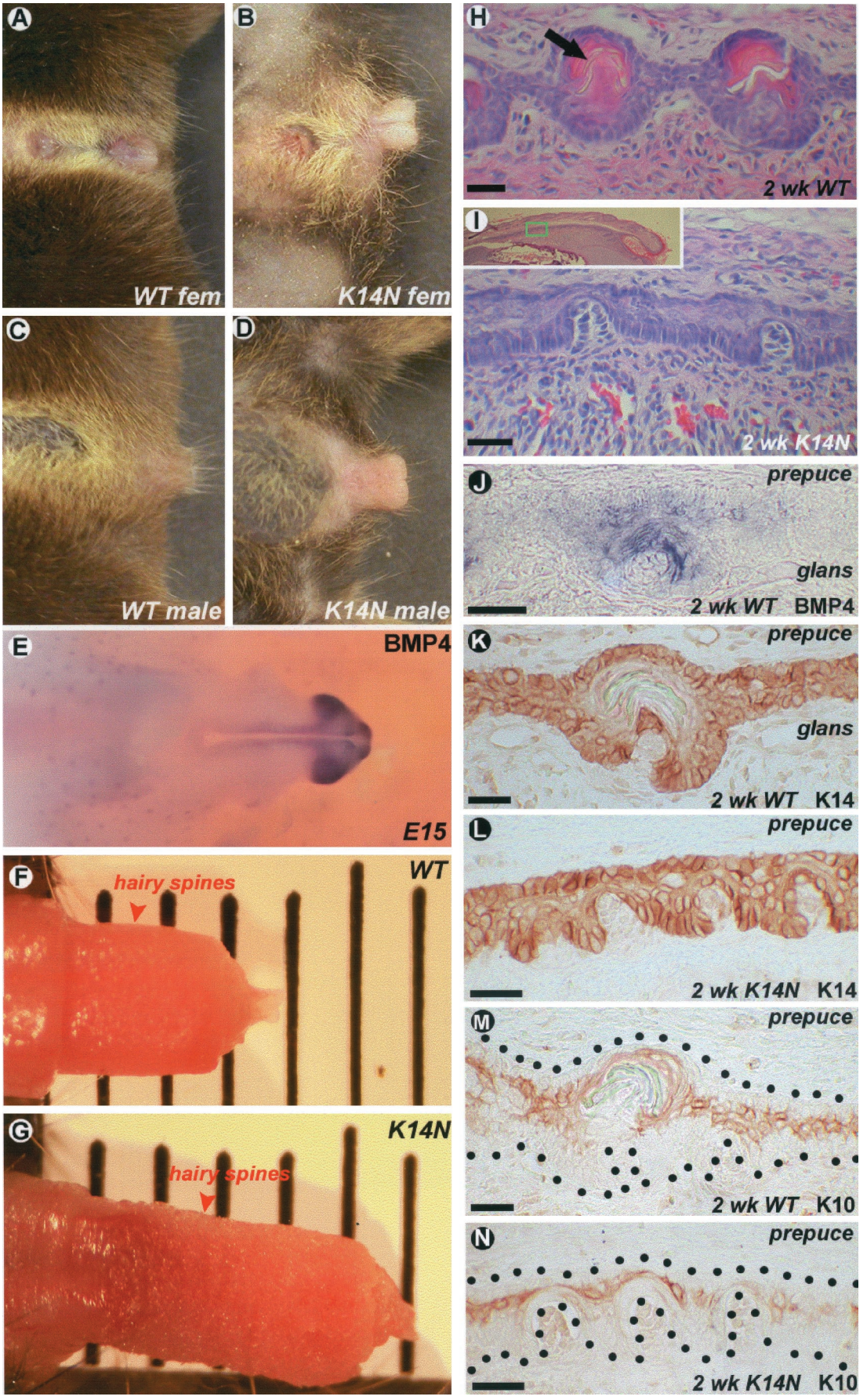
A
WT fem
B
K14N fem
C
WT male
D
K14N male
E
BMP4
E15
F
hairy spines
WT
G
hairy spines
K14N
H
2 wk WT
I
2 wk K14N
J
prepuce
glans
2 wk WT BMP4
K
prepuce
glans
2 wk WT K14
L
prepuce
2 wk K14N K14
M
prepuce
2 wk WT K10
N
prepuce
2 wk K14N K10

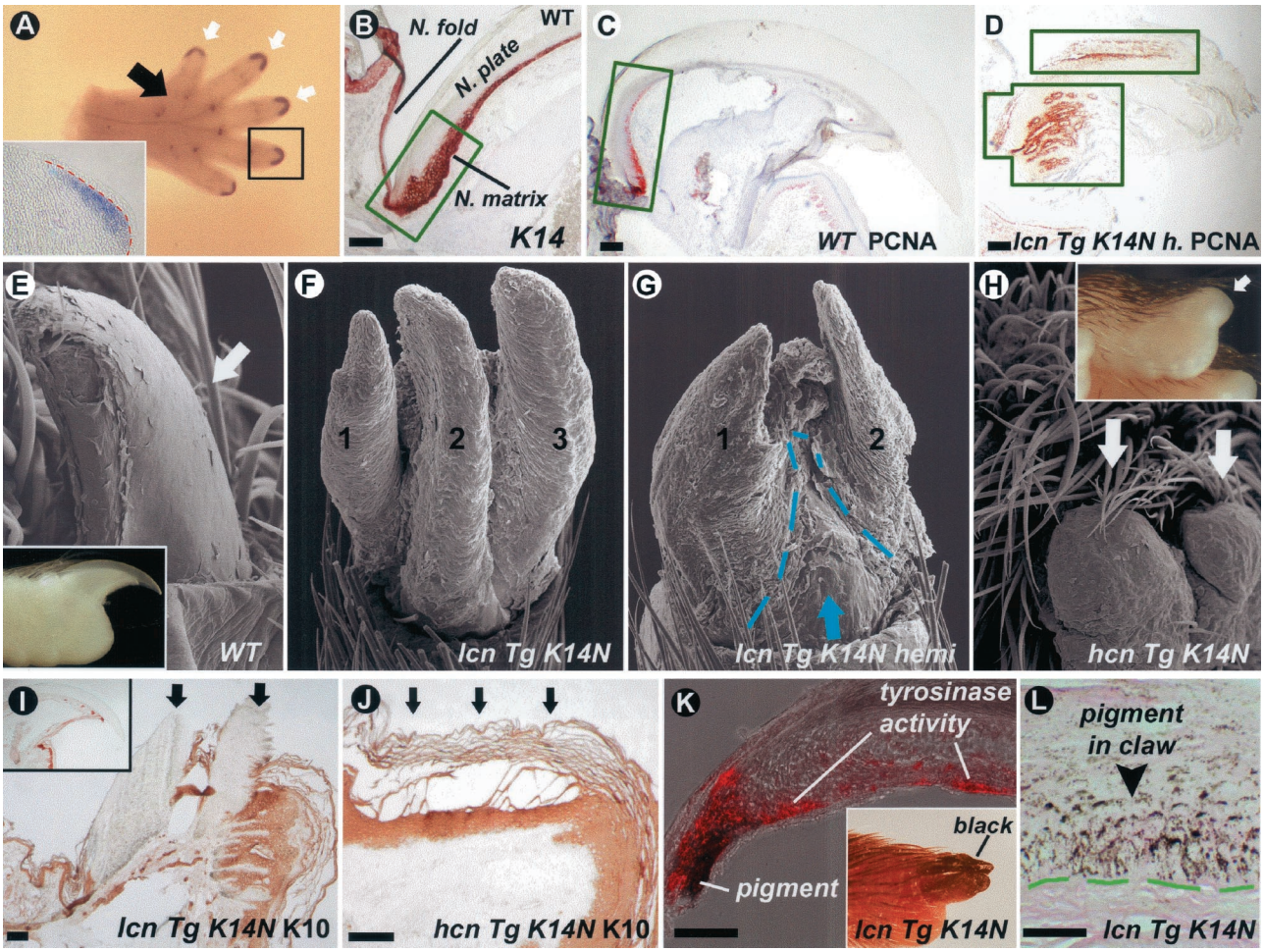

Figure 5. Pathology in claws. **A:** E15 wild-type mouse paw *in situ* with BMP4 probe. **White arrows** point to expression sites at the tips of the digits. **Black arrow** points to the group of expression sites corresponding to footpads. BMP4 expression in the mesenchyme of the developing claw is shown on the **inset**. **B:** Strong K14 expression in epithelial cells of proliferating claw matrix (**green box**) and beyond it. **C** and **D:** Expansion of proliferating area in the claw of low-TG copy number K14-Noggin mice (lcn TG K14-Noggin mice). PCNA-positive cells are limited to the claw matrix (**green box**) in wild-type mice, but extend all of the way to the tip of the digit in K14-Noggin mice (**green boxes**). There are multiple proliferating centers within one claw of the K14-Noggin mice. **E** to **H:** Progressive abnormalities in the claw of the K14-Noggin mice. Compared to the control claw from C57BL/6J mouse (**E**), claws in the low-TG copy number K14-Noggin mice split into separate plates (**F**) and are partially substituted by epidermis (**G**, demarcated with a **green dotted line**). No claw is identifiable in the high-TG copy number K14-Noggin mice (**H**, **white arrows**). **I** and **J:** K10 keratin expression in low (**I**) and high (**J**) TG copy number K14-Noggin mice. In low-TG copy number mice claws are K10-negative (**arrows**) despite the apparent macroscopic and microscopic abnormalities (see above). In the high-TG copy number mouse the epidermis that substitutes the claw expresses K10 (**arrows**). In the control mouse (**K**, **inset**) the claw is K10-negative. **K** and **L:** Pigmentation of the claw in low-TG copy number K14-Noggin mice. Abundant pigment deposits in the claw epithelium (**L**). Tyrosinase activities (red color, **K**) associated with pigment production are seen. Scale bars: 100 μm (**B–D** and **I–K**); 25 μm (**L**).

pigmented (Figure 5K, inset). On histological sections, unlike in the control mice, basal and suprabasal layers of claws from K14-Noggin mice contained abundant melanin granules (Figure 5L). Tyrosinase activity, a general marker of melanocytes, was detected in the pigmented claws (Figure 5K).

Ventral Paw

There are several changes in the ventral paw integuments in high-TG copy number and low-TG copy number K14-Noggin mice. Normally there are six footpads (Figure 6A) that have evolved for land habitats.[47] BMPs are specifically expressed in the footpads. At E15, developing footpad areas showed localized BMP4 expression in the mesenchyme (Figure 6E). At later developmental stages and in adults BMPs expression shifts to the epidermis. Both BMP2 and BMP4 are specifically expressed in the footpads' epidermis and are down-regulated in the epidermis outside of the footpads (Figure 6, F and G). K14 is expressed in the epidermis of developing footpads (Figure 6I). Localized proliferation in the mesen-

Figure 4. Pathology in external genitalia. **A** and **B:** External genitalia of the control and K14-Noggin female mice. **C** and **D:** External genitalia of the control and K14-Noggin male mice. **E:** BMP4 expression pattern in the external genitalia of E15 mouse embryo. Very strong expression in the glans penis. **F** and **G:** Side-to-side comparison of the control and K14-Noggin male external genital. **H** and **I:** Hairy spines of the 2-week-old control and K14-Noggin mice. Hairy spines in the K14-Noggin mouse are not completely developed. **J:** BMP4 expression in the developing hairy spine of the 2-week-old control mouse. **K–N:** K14 and K10 keratin expression patterns in the preputial lamella and developing hairy spines on the border of the glans and prepuce from a 2-week-old wild-type and K14-Noggin mouse. Note weak K10 expression in the immature hairy spines of the K14-Noggin mouse (**N**). Scale bars 25 μm.

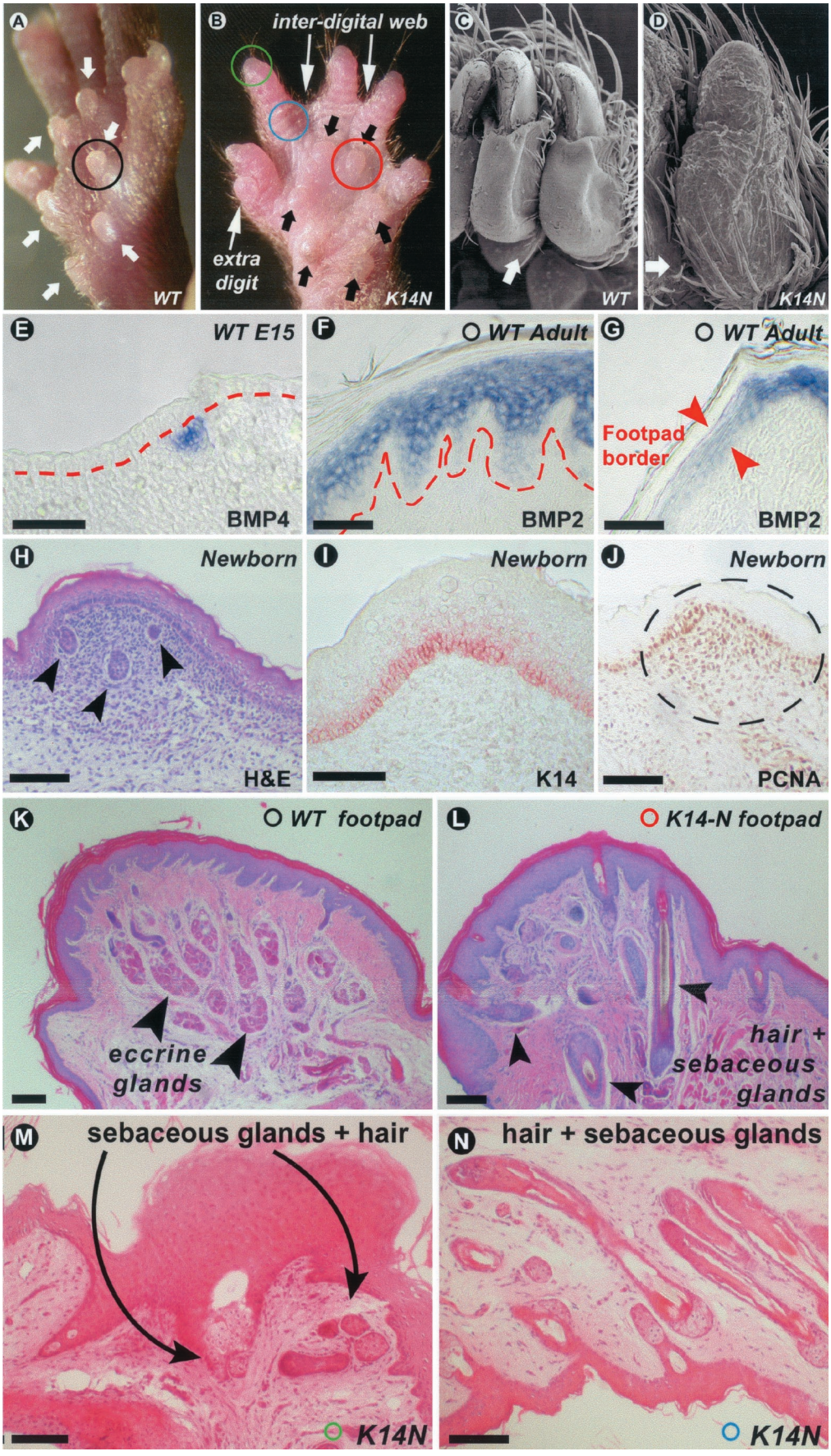
A
WT
B
inter-digital web
extra digit
K14N
C
WT
D
K14N
E
WT E15
BMP4
F
WT Adult
BMP2
G
WT Adult
Footpad border
BMP2
H
Newborn
H&E
I
Newborn
K14
J
Newborn
PCNA
K
WT footpad
eccrine glands
L
K14-N footpad
hair + sebaceous glands
M
sebaceous glands + hair
K14N
N
hair + sebaceous glands
K14N

chyme results in footpad growth (Figure 6, H and J). In high-TG copy number K14-Noggin mice, footpads are hypoplastic (Figure 6B). Footpads in mutant mice are markedly shallower, but the total number of footpads do not change.

Normally, the ventral paw has glabrous skin and does not contain any significant amount of hairs (Figure 6C). Footpads are completely devoid of hairs (Figure 6K). The ventral paw skin contains eccrine glands, which are particularly dense at the tip of the digits and in the footpads (Figure 6K). In contrast, numerous HFs in high-TG copy number K14-Noggin mice were found on the ventral side of the paws, including footpads where we observed nearly complete substitution of eccrine glands by HFs (Figure 6; L to N).

Discussion

The formation of ectodermal organs depends on a series of topological transforming activities of the epithelial sheet such as folding, thickening, branching, and so forth. These processes are based on local cellular behaviors including proliferation, differentiation, re-arrangement, and apoptosis. The formation of all ectodermal organs goes through induction, morphogenesis, and differentiation stages. In addition, some ectodermal organs undergo cycling/regeneration stages.[48] They share fundamental signaling pathways during these developmental stages and thus they are variations overlaid on the common theme.[49,50] Serious defects of these basic signaling pathways tend to generate multiple ectodermal organ defects as seen in some forms of ectodermal dysplasia.[51] Milder perturbation of the strength of these pathway activities may lead to morphoregulation, ie, the modulation of the morphological phenotype of the organ.[52] Here we further propose that when the perturbation mainly acts during induction stages, the total number of a given ectodermal organ is altered. In contrast, when the perturbation mainly acts during morphogenesis stages, the size and shape of the organ may change. Finally, when perturbation acts mainly during differentiation stages, maturation of the organ is affected.

We tried to modulate one of the molecular pathways to evaluate the validity and the scope of this model. We analyzed the multiple roles of the BMP pathway in ectodermal organ morphogenesis using K14-Noggin mice. The onset of transcriptional activation of keratin 14 and its partner keratin 5 was studied previously.[53] It was shown that their transcription was first detected as early as E9.5. At early times, expression is restricted to certain areas of the embryo, such as the ectoderm of the developing

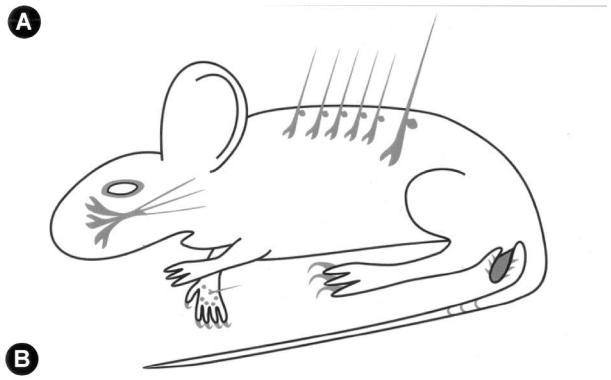

	Phenotypes of K14-Noggin mice		
	Stages		
	Induction	Morphogenesis	Differentiation
Eyelids	Formation of extra cilia at the expense of the Miebomian glands	Defective eyelids opening. Small eye opening	
Vibrissae	Induction of extra follicles, formation of compound vibrissa follicles		
Pelage hair	Induction of extra secondary hair follicles, predominantly awl and auchene. Hypertrophic hair follicles		
Eccrine glands in the ventral paw skin and footpads	Pilosebaceous units replace sweat glands		
Interdigital spacing		Failure of the digits separation. Webbing in between digits	
Footpads		Formation of smaller footpads	
Claws	Induction of claws fails. Absence of claws (High TG copy number mice)	Formation of multiple claw plates within one claw field (low Tg copy number mice)	Incomplete differentiation and pigmentation of claw plates (low Tg copy number mice)
External genitalia		Larger external genitalia both in males and females	Retarded differentiation of hairy spines
Interfollicular epidermis			Hyperplasia of the epidermis

Figure 7. Summary of multiple epidermal organ defects caused by disruption of BMP pathway in the skin. **A:** Defective regions are shown in gray shades. **B:** Phenotypes are summarized. They are grouped based on the developmental stages when defects occur.

facial structures. At E13.5 to E14.5, there is a dramatic increase and expansion of K14 and K5 promoter activity in ectoderm throughout the body of the embryo. This coincides or precedes development of the ectodermal organs affected in K14-Noggin mice by overexpressed Noggin. However, the minimal concentration of Noggin required to perturb a particular ectodermal organ can be reached during induction, morphogenesis, or differentiation stages of that particular organ, thus producing different phenotypes. In several occasions, rather than producing serious pathological changes with functional impairment, Noggin altered ectodermal organ number, size, and differentiation status. Here, we focus on the multiple ectodermal organ defects caused by suppression of the BMP pathway (Figure 7), and

Figure 6. Pathology of the ventral side of the paw. **A** and **B:** Normal and hypoplastic foot pads from the wild-type and K14-Noggin mouse, respectively (**white** and **black arrows**). Presence of additional digit and interdigital webbing are marked in K14-Noggin mouse paw. **C** and **D:** Scanning EM normal glabrous skin and skin with ectopic HFs on the ventral side of the digits from wild-type and K14-Noggin mice, respectively. **E:** BMP4 expression in the mesenchyme of the developing footpad in E15 control mouse embryo. **F** and **G:** Suprabasal expression of BMP2 in the epidermis of the adult footpad (**F**) and on the border of the footpad (**G**). Note the sharp decline of BMP2 expression on the border of the footpad. **H** to **J:** Growing footpad of the newborn mouse. Active proliferation is seen in the mesenchymal condensation of the footpad as judged by PCNA staining (**J**). Eccrine glands are forming at this time (marked by **arrowheads** at **H**). K14 is expressed in the basal layer of the footpad epidermis (**I**). **K** and **L:** H&E of the footpad from control and K14-Noggin mice. Typical afollicular epidermis and eccrine glands are seen in the control mouse (**K**). In the K14-Noggin mouse, multiple HFs replace the eccrine glands. **M** and **N:** H&E of the skin on the digit from K14-Noggin mouse. **M:** Tip of the digit. Claw is absent. It is substituted by a hyperplastic patch of epidermis with sebaceous glands and HFs. **N:** Ventral side of the distal digit. Many HFs with sebaceous glands have formed, instead of sweat glands and just a few HFs in the normal. Scale bars, 100 μm.

discuss the concept of pathological changes and phenotypic variations.

BMP Regulates the Number, Size, Type, and Cycling of HFs

In the adult mouse, two types of hairs can be found: primary (tylotrich) and secondary (nontylotrich). Secondary hairs are further classified into awl, auchene, and zigzag based on the shaft structure. Primary and secondary HFs start to develop at E14.5 and E16.5 accordingly during embryogenesis,[54–56] and may depend on different molecular pathways.[3] Primary HF morphogenesis is highly dependent on the Eda pathway.[57] Secondary HF morphogenesis is highly dependent on the level of BMPs and their antagonists, such as Noggin. Using the Noggin-knockout mouse model, it was previously shown that excessive amounts of BMP leads to the inhibition of the secondary, but not primary HF formation.[27]

Our results indicate that excess of Noggin affects hair induction and results in an increase in HF density by up to 80%. Primarily the number of secondary awl and auchene hairs are increased. This is consistent with the idea that BMPs/Noggin specifically control and modulate secondary HF formation. Noggin may result in a higher density of HFs in two ways. First, by lowering the threshold for the induction of awl and auchene HFs, and second, by lengthening the competence period and extending the inductive phase of these HFs further into postnatal life.

New HFs can be induced from interfollicular epidermis or from the outer root sheath of the pre-existing HFs, as in the case of compound follicles.[45] Compound HF formation was observed in K14-ΔN87βcat mice that express a stabilized form of β-catenin under the K14 promoter. In K14-ΔN87βcat mice, supernumerary HF formation takes place continuously throughout postnatal life and is associated with pilomatricoma formation in the skin.[31] In the K14-Noggin mice, induction of new pelage HFs primarily occurred in the interfollicular epidermis. However in vibrissae, we observed many compound follicles as they all share one infudibulum and outer root sheath. We propose that the presence of Noggin lowers the threshold for the induction allowing additional HFs to be induced from the interfollicular epidermis or the outer root sheath. Using the same reasoning, ectopic HFs were induced from the glaborous skin of the ventral paws including footpads. Previously, it was reported that adult dermal papillae transplanted under glabrous epidermis could induce new HF formation.[58,59] The adult dermal papilla is a strong site of Noggin signaling,[25] and Noggin may be responsible in part for the inductive abilities of the dermal papillae.

Noggin shows a distinct spatio-temporal distribution during hair development. During development at E15.5 to E17.5 Noggin is expressed in the mesenchyme underneath the epidermis. In the adult mouse, its expression is restricted to the dermal papillae.[25] Broad Noggin expression at E15.5 to E17.5 in the skin coincides with induction of nontylotrich HFs. Mesenchymally derived Noggin competes with BMP2, four ligands for binding to BMPR-IA in hair placodes. In our mouse model, excessive Noggin produced in the epidermis under the K14 promoter strongly inhibited BMP2 and BMP4 signaling during the crucial time of HF formation. Therefore, the activator/inhibitor ratio in the microenvironment was tilted toward the activator resulting in additional HFs.

Hairs in K14-Noggin mice cycled significantly faster than in control mice. Although there was no significant change in the length of the anagen, the telogen in K14-Noggin mice was markedly shorter than the telogen observed in control mice. Our observation is consistent with the effect of exogenous Noggin delivery into the telogen skin on wild-type mice. Implantation of beads soaked with Noggin results in hair growth induction.[60] Our results add to the evidence that the BMP pathway is an important regulator of the telogen-anagen transition.

BMP Affects the Development of Claw and Integuments of the Distal Limbs

In the paw of K14-Noggin mice, we observed syndactyly and postaxial polydactyly, consistent with what was reported previously.[46] In K14-Noggin mice, the induction, morphogenesis, and differentiation stages are affected. Claw agenesis was seen in high-TG copy number mice. The claw induction failed and the claw fields underwent alternative epidermal differentiation. Low-TG copy number mice developed aberrant claws. During the morphogenesis stage the original claw field splits into several claw plates, but they remain in the same plane. At later differentiation stages, these claws show abnormal differentiation with loss of function. Claw morphology and differentiation is affected because claw matrix cells are K14-positive. An excess of Noggin in the claw matrix affects normal proliferation and delays claw-specific differentiation. Localized zone of proliferating cells normally located next to the eponychium is expanded and proliferating cells, in isolated patches, are present all of the way toward the tip of the claw in K14-Noggin mice. It is interesting to note that claw malformation was also reported for the Msx2-Noggin transgenic mouse[34] and Msx2 is known to be expressed in the claw area (our data, not shown). However the Msx2-Noggin claw phenotype was not described in full to allow comparison with the K14-Noggin phenotype.

Hyperpigmentation of the claws is a prominent feature of K14-Noggin mice. In mouse skin, active melanogenesis occurs only in the matrix of anagen HFs. Stem cell factor is expressed in epithelial cells of the hair matrix and is important for stimulating melanogenesis.[61] If stem cell factor is constitutively expressed under the K14 promoter, the epidermis becomes pigmented.[62] We speculate that Noggin may up-regulate the stem cell factor in the claw, thus causing activation of melanogenesis.

Footpads displayed major modifications in the ventral paw.[47] Localized mesenchymal cell proliferation is a key event during footpad development.[63] Epidermal thickening and eccrine sweat gland formation accompanies mesenchymal expansion. Excess of Noggin results in

hypoplastic footpads. Noggin suppresses localized mesenchymal cell proliferation that is otherwise positively controlled by BMPs. Noggin also suppresses eccrine sweat glands and causes formation of pilosebaceous units. Noggin may abrogate the induction of sweat glands and induce HFs as alternative skin appendages, or they may *trans*-differentiate the induced early sweat gland primordia into hairs.

BMP Decreases the Size of Eyelid Opening

The morphogenetic process for the opening of the eyelids is affected in K14-Noggin mice. This leads to small eye openings and abnormally shaped eyelids, especially obvious in lateral and medial commissures. Excessive Noggin also suppresses induction of Meibomian glands and induces formation of many ectopic cilia often pointing inwards toward the cornea. The extent of these pathological changes is highly dependent on the transgene copy number. Severe eyelid abnormalities were seen only in mice with a high level of K14-Noggin as judged by real-time quantitative PCR. The eyelid opening process is not delayed in our K14-Noggin mice, but the eyelid opening is smaller. Recently, BMP pathway was proposed to be involved in the timing of eyelid opening.[64] On a K5-Noggin background, the eyelid opening was delayed by 20 days, and the suppression by Noggin on eyelid apoptosis and differentiation was proposed to be a possible mechanism. Also, keratin 14 is reported to be partially replaced by keratin 15. In our K14-Noggin mice, the level of keratin 14 expression is not diminished in the eye suture in comparison to the back skin. However, no abnormalities of the adult eyelid were described in the K5-Noggin mice.

BMP Regulates the Size of External Genitalia and Integument Differentiation

External genitalia form from the genital tubercle. The genital tubercle differentiates into the penis in males or clitoris in females.[65,66] The formation of the genital tubercle, its outgrowth and differentiation into either penis or clitoris is the result of epithelial-mesenchymal interaction.[67] In both males and females, external genital outgrowth is accomplished by the formation of the prepuce. WNT, SHH, and FGF signaling were shown to be involved in genital morphogenesis.[68–70] Thus, external genitalia are another example of ectodermal organs regulated by a similar set of morphogenesis-related signaling molecules.

Here we show BMPs, in particular BMP4, to be expressed at the tip of the genital tubercle where growth may be regulated. K14-Noggin mice of both genders show excessive outgrowth of the external genitalia, which is especially apparent in the postnatal period. We suggest that BMP signaling regulates the growth of penile and clitoral tissues in mice, and that ectopic Noggin disrupts the balanced growth of these structures and results in their hypertrophy.

In mice there are hairy spines, which are epithelial appendages of the glans penis with possible mechanosensory function. Their formation starts around P10 and it was shown to be androgen-dependent, because it is primarily retarded in androgen-insensitive mice.[71] Here we showed that BMPs are expressed within the epithelium of developing hairy spines and control their differentiation. Excessive Noggin in the basal layer of the preputial lamellae inhibits hairy spine maturation, but not the number of hairy spines. Therefore, BMP signaling is important for the differentiation of hairy spines, but not for their induction and periodic arrangement.

BMP and Human Diseases

The BMP pathway is of fundamental importance for early stages of development.[72] Therefore, all mutations of BMPs are likely to be lethal. Noggin is a direct antagonist of BMPs. Human loss-of-function mutations in the Noggin gene (NOG) were reported. Affected people have fusion of the joints (proximal symphalangism, SYM1) or multiple-synostoses syndrome (SYNS1) and conductive deafness, because of stapes ankylosis.[73,74] To date, no known gain-of-function NOG gene mutations are known. However, if they exist, theoretically these mutations should result in phenotypes similar to that of a hypothetical BMP-knockout human. We have searched for human congenital anomalies associated with a locus at 17q22, because human NOG is mapped to this area of chromosome 17.[75] We found that several phenotypical features of people with chromosome 17q trisomy syndrome [mental retardation (MCA/MR) syndrome] resemble those found in K14-Noggin mice.[76,77] These include: polydactyly of the hands and feet, syndactyly of the fingers and toes; hirsutism, a widow's peak (low, v-shaped hair growth near the top of the human forehead), low posterior hairline, and external genital abnormalities including a bifid scrotum and penile chordae. These abnormalities parallel the paw abnormalities, hypertrichosis, and external genital abnormalities seen in K14-Noggin mice. We speculate that a higher dosage of Noggin, resulting from an additional NOG gene allele in people with 17q trisomy is partially responsible for the above-mentioned abnormalities.

Morpho-Regulation: Variations or Pathology?

Although some phenotypic features are pathological and result in loss-of-function (absence or aberrant claws, replacement of eccrine glands in paw and Meibomian glands in eyelids with hair), many changes are relatively mild and mostly regulatory in nature. These changes seem to be quantitative (eg, an increase in pelage hair density), qualitative (eg, reduction of the size of footpads), or functional (eg, shorter telogen). Although all these changes are still considered abnormal because they indeed significantly deviate from the normal average phenotypes, it may be worthwhile to contemplate the borders between pathology and phenotypic variations.

The concept of morpho-regulation implies that morphogenetic processes can be modulated by morphological regulators that lead to changes of morphological phenotypes in development and in evolution.[52] Because the levels of morpho-regulators can be adjusted physiologically, they provide means for modulating the morphology of organs without drastic changes. Whereas Edelman[52] concentrated on cell adhesion molecules as morpho-regulators, here we develop this concept further to major morphogenesis signaling pathways (eg, BMP, Wnt, Shh, FGF pathways) and their modulation by physiological antagonists. Using the pliable BMP pathway as an example, this genetically engineered mouse illustrates the morpho-regulatory hypothesis vividly.

In the context of evolution, the term phenotypic plasticity is used to describe the ability of a phenotype to shift quantitatively.[78] At the level of species, it may be based on the selection from a spectrum of phenotypic variations based on environmental changes. Examples are seen in the different densities and length of hairs observed in mountain cats, dogs, oxen, and so forth, from temperate or extremely cold areas found in arctic or high mountain regions,[79] or the shift of finch beak shapes in accord to climate changes in Galapagos islands.[80] Variations in the number and size of integumentary appendages can be used to generate a spectrum of variable animal phenotypes that may work as substrates for selection and become advantageous when environments change. However, when these morphological or structural variations impede normal functions, they will be considered pathological.

The recognition that accumulation of mild mutations or variations can result in the formation of a new trait or new species is not new,[78] but candidate molecular pathways responsible for these variations are mostly unknown. Here we show Noggin/BMP antagonism may serve this mechanism. Further study on a more quantitative and more regulatory level is needed to develop this concept further. In this case, integument appendages constitute an ideal model because their changes are usually nonlethal (eg, unlike many changes affecting heart or lung) and are easier to be quantified.[81]

This study shows how simple tuning up and down of the key molecular pathways activity, such as the BMP, may regulate the formative process of ectodermal organs. In the era of tissue engineering, one may want to modulate the number, size, or the differentiation status of some ectodermal organs in humans or animals for various medical, agricultural, and industrial reasons. Tissue engineers will have to learn how to accomplish the subtle balance of activities for the major signaling pathways. The newly made transgenic mouse can be a useful animal model and tissue source for these analyses and evaluations.

Acknowledgments

We thank Ms. Marijane Ramos and Ms. Fiona McCulloch for help with manuscript preparation; Dr. Yan Zhang for technical assistance; Dr. Sundberg for advice in hair research; Dr. Gen Yamada for helpful comments on external genitalia; Dr. Norman W. Marten and Dr. Jiehao Zhou for their help in setting up real-time quantitative PCR assay and interpretation of the results; Dr. Mingke Yu and Mr. Marcus Medina for help in setting up the tyrosinase assay; and Michelle MacVeigh, from the Microscopy Sub Core at the University of Southern California Center for Liver Diseases, for her help with fluorescent microscopy.

References

1. Chuong C-M (Ed): Molecular Basis of Epithelial Appendage Morphogenesis. Austin, Landes Bioscience, 1998
2. Wisniewski SA, Kobielak A, Trzeciak WH, Kobielak K: Recent advances in understanding of the molecular basis of anhidrotic ectodermal dysplasia: discovery of a ligand, ectodysplasin A and its two receptors. J Appl Genet 2002, 43:97–107
3. Headon DJ, Overbeek PA: Involvement of a novel Tnf receptor homologue in HF induction. Nat Genet 1999, 22:370–374
4. Brunner HG, Hamel BC, Bokhoven HVH: P63 gene mutations and human developmental syndromes. Am J Med Genet 2002, 112:284–290
5. Chuong C-M, Chodankar R, Widelitz RB, Jiang TX: Evo-devo of feathers and scales: building complex epithelial appendages. Curr Opin Dev Genet 2000, 10:449–456
6. Fuchs E, Merrill BJ, Jamora C, DasGupta R: At the roots of a never-ending cycle. Dev Cell 2001, 1:13–25
7. Botchkarev VA: Bone morphogenetic proteins and their antagonists in skin and HF biology. J Invest Dermatol 2003, 120:36–47
8. Reddi AH: Role of morphogenetic proteins in skeletal tissue engineering and regeneration. Nat Biotechnol 1998, 16:247–252
9. Miyazono K, Kusanagi K, Inoue H: Divergence and convergence of TGF-beta/BMP signaling. J Cell Physiol 2001, 187:265–276
10. Wozney JM: Overview of bone morphogenetic proteins. Spine 2002, 27:S2–S8
11. Itoh S, Itoh F, Goumans MJ, Ten Dijke P: Signaling of transforming growth factor-beta family members through Smad proteins. Eur J Biochem 2000, 267:6954–6967
12. Piscione TD, Phan T, Rosenblum ND: BMP7 controls collecting tubule cell proliferation and apoptosis via Smad1-dependent and -independent pathways. Am J Physiol 2001, 280:F19–F33
13. Massague J, Chen YG: Controlling TGF-beta signaling. Genes Dev 2000, 14:627–644
14. Zimmerman LB, De Jesus-Escobar JM, Harland RM: The Spemann organizer signal Noggin binds and inactivates bone morphogenetic protein 4. Cell 1996, 86:599–606
15. Piccolo S, Agius E, Lu B, Goodman S, Dale L, De Robertis EM: Cleavage of chordin by xolloid metalloprotease suggests a role for proteolytic processing in the regulation of Spemann organizer activity. Cell 1997, 91:407–416
16. Yamaguchi K, Nagai S, Ninomiya-Tsuji J, Nishita M, Tamai K, Irie K, Ueno N, Nishida E, Shibuya H, Matsumoto K: XIAP, a cellular member of the inhibitor of apoptosis protein family, links the receptors to TAB1-TAK1 in the BMP signaling pathway. EMBO J 1999, 18:179–187
17. Panchision DM, Pickel JM, Studer L, Lee S-H, Turner PA, Hazel TG, McKay RDG: Sequential actions of BMP receptors control neural precursor cell production and fate. Genes Dev 2001, 15:2094–2110
18. Kimura N, Matsuo R, Shibuya H, Nakashima K, Taga T: BMP2-induced apoptosis is mediated by activation of the TAK1–p38 kinase pathway that is negatively regulated by Smad6. J Biol Chem 2000, 275:17647–17652
19. Zhang H, Bradley A: Mice deficient for BMP2 are nonviable and have defects in amnion/chorion and cardiac development. Development 1996, 122:2977–2986
20. Wilson PA, Hemmati-Brivanlou A: Induction of epidermis and inhibition of neural fate by Bmp-4. Nature 1995, 376:331–333
21. Lyons KM, Pelton RW, Hogan BL: Patterns of expression of murine Vgr-1 and BMP-2a RNA suggest that transforming growth factor-beta-like genes coordinately regulate aspects of embryonic development. Genes Dev 1989, 3:1657–1668

22. Wall NA, Blessing M, Wright CV, Hogan BL: Biosynthesis and in vivo localization of the decapentaplegic-Vg-related protein, DVR-6 (bone morphogenetic protein-6). J Cell Biol 1993, 120:493–502
23. Takahashi H, Ikeda T: Transcripts for two members of the transforming growth factor-beta superfamily BMP-3 and BMP-7 are expressed in developing rat embryos. Dev Dyn 1996, 207:439–449
24. Bitgood MJ, McMahon AP: Hedgehog and Bmp genes are coexpressed at many diverse sites of cell-cell interaction in the mouse embryo. Dev Biol 1995, 172:126–138
25. Botchkarev VA, Botchkareva NV, Roth W: Noggin is a mesenchymally-derived stimulator of HF induction. Nat Cell Biol 1999, 1:158–164
26. Noramly S, Morgan BA: BMPs mediate lateral inhibition at successive stages in feather tract development. Development 1998, 125:3775–3787
27. Botchkarev VA, Botchkareva NV, Sharov AA, Funa K, Huber O, Gilchrest BA: Modulation of BMP signaling by Noggin is required for induction of the secondary (nontylotrich) HFs. J Invest Dermatol 2002, 118:3–10
28. Blessing M, Nanney LB, King LE, Jones CM, Hogan BL: Transgenic mice as a model to study the role of TGF-beta-related molecules in HFs. Genes Dev 1993, 7:204–215
29. Kulessa H, Turk G, Hogan BL: Inhibition of Bmp signaling affects growth and differentiation in the anagen HF. EMBO J 2000, 19:6664–6674
30. Zhou P, Byrne C, Jacobs J, Fuchs E: Lymphoid enhancer factor 1 directs HF patterning and epithelial cell fate. Genes Dev 1995, 9:700–713
31. Gat U, DasGupta R, Degenstein L, Fuchs E: De novo HF morphogenesis and hair tumors in mice expressing a truncated β-catenin in skin. Cell 1998, 95:605–614
32. Huelsken J, Vogel R, Erdmann B, Cotsarelis G, Birchmeier W: Beta-catenin controls HF morphogenesis and stem cell differentiation in the skin. Cell 2001, 105:533–545
33. Andl T, Reddy ST, Gaddapara T, Millar SE: WNT signals are required for the initiation of HF development. Dev Cell 2002, 2:643–653
34. Jamora C, DasGupta R, Kocieniewski P, Fuchs E: Links between signal transduction, transcription and adhesion in epithelial bud development. Nature 2003, 422:317–322
35. Vassar R, Fuchs E: Transgenic mice provide new insights into the role of TGF-alpha during epidermal development and differentiation. Genes Dev 1991, 5:714–727
36. Liu YH, Ma L, Wu LY, Luo W, Kundu R, Sangiorgi F, Snead ML, Maxson R: Regulation of the Msx2 homeobox gene during mouse embryogenesis: a transgene with 439 bp of 5′ flanking sequence is expressed exclusively in the apical ectodermal ridge of the developing limb. Mech Dev 1994, 48:187–197
37. Dhar AK, Roux MM, Klimpel KR: Detection and quantification of infectious hypodermal and hematopoietic necrosis virus (IHHNV) and white spot virus (WSV) of shrimp by real-time quantitative PCR and SYBR chemistry. J Clin Microbiol 2001, 39:2835–2845
38. Hizer SE, Dhar AK, Klimpel KR, Garcia DK: RAPD markers as predictors of infectious hypodermal and hematopoietic necrosis virus (IHHNV) resistance in shrimp (Litopenaeus stylirostris). Genome 2002, 45:1–7
39. Han R, Baden HP, Brissette JL, Weiner L: Redefining the skin's pigmentary system with a novel tyrosinase assay. Pigment Cell Res 2002, 15:290–297
40. Jiang TX, Jung HS, Widelitz RB, Chuong CM: Self-organization of periodic patterns by dissociated feather mesenchymal cells and the regulation of size, number and spacing of primordia. Development 1999, 126:4997–5009
41. Millar SE, Willert K, Salinas PC, Roelink H, Nusse R, Sussman DJ, Barsh GS: WNT signaling in the control of hair growth and structure. Dev Biol 1999, 207:133–149
42. Nakamura M, Sundberg JP, Paus R: Mutant laboratory mice with abnormalities in hair follicle morphogenesis, cycling, and/or structure: annotated tables. Exp Dermatol 2001, 10:369–390
43. Slominski A, Paus R, Plonka P, Chakraborty A, Maurer M, Pruski D, Lukiewicz S: Melanogenesis during the anagen-catagen-telogen transformation of the murine hair cycle. J Invest Dermatol 1994, 102:862–869
44. Oro AE, Higgins K: Hair cycle regulation of Hedgehog signal reception. Dev Biol 2003, 255:238–248
45. Moore GP, Jackson N, Isaacs K, Brown G: Pattern and morphogenesis in skin. J Theor Biol 1998, 191:87–94
46. Guha U, Gomes WA, Kobayashi T, Pestell RG, Kessler JA: In vivo evidence that BMP signaling is necessary for apoptosis in the mouse limb. Dev Biol 2002, 249:108–120
47. Hamrick MW: Evolution and development of mammalian limb integumentary structures. J Exp Zool, Part B, Mol Dev Evol 2003, 298:152–163
48. Wu T, Chuong C-M: Developmental biology of skin appendages. Hair Biology and Disorders: Research, Pathology and Management. Edited by F Camacho, VA Randall, VH Price. London, Martin Dunitz, 2000, pp 17–37
49. Chuong CM, Noveen A: Phenotypic determination of epithelial appendages: genes, developmental pathways, and evolution. J Invest Dermatol Symp Proc 1999, 4:307–311
50. Chuong C-M, Lin S-L, Patel N, Jung H-S, Widelitz RB: Sonic Hedgehog signaling pathway in vertebrate ectodermal organ formation: perspectives in development and evolution. Cell Mol Life Sci 2000, 57:1672–1681
51. Slavkin HC, Shum L, Nuckolls GH: Ectodermal dysplasia: a synthesis between evolutionary, developmental, and molecular biology and human clinical genetics. Molecular Basis of Epithelial Appendage Morphogenesis. Edited by CM Chuong. Austin, Landes Bioscience, 1998
52. Edelman GM: Morphoregulation. Dev Dyn 1992, 193:2–10
53. Byrne C, Tainsky M, Fuchs E: Programming gene expression in developing epidermis. Development 1994, 120:2369–2383
54. Vielkind U, Hardy MH: Changing patterns of cell adhesion molecules during mouse pelage HF development. 2. Follicle morphogenesis in the hair mutants, tabby and downy. Acta Anat 1996, 157:183–194
55. Philpott MP, Paus R: Principles of HF morphogenesis. Molecular Basis of Epithelial Appendage Morphogenesis. Edited by CM Chuong. Austin, Landes Bioscience, 1998, pp 75–103
56. Paus R, Cotsarelis G: The biology of HFs. N Engl J Med 1999, 341:491–498
57. Laurikkala J, Pispa J, Jung HS, Nieminen P, Mikkola M, Wang X, Saarialho-Kere U, Galceran J, Grosschedl R, Thesleff I: Regulation of HF development by the TNF signal ectodysplasin and its receptor Edar. Development 2002, 129:2541–2553
58. Jahoda CA, Reynolds FJ: Cultured dermal papilla cells induce follicle formation and hair growth by transdifferentiation of an adult epidermis. Development 1992, 115:587–593
59. Jahoda CA, Reynolds AJ: Dermal-epidermal interaction. Follicle derived cell populations in the study of hair growth mechanism. J Invest Dermatol 1993, 101:33s–38s
60. Botchkarev VA, Botchkareva NV, Nakamura M, Huber O, Funa K, Lauster R, Paus R, Gilchrest BA: Noggin is required for induction of the HF growth phase in postnatal skin. EMBO J 2001, 15:2205–2214
61. Botchkareva NV, Khlgatian M, Longley BJ, Botchkarev VA, Gilchrest BA: SCF/c-kit signaling is required for cyclic regeneration of the hair pigmentation unit. EMBO J 2001, 15:645–658
62. Nishimura EK, Jordan SA, Oshima H, Yoshida H, Osawa M, Moriyama M, Jackson IJ, Barrandon Y, Miyachi Y, Nishikawa S: Dominant role of the niche in melanocyte stem-cell fate determination. Nature 2002, 416:854–860
63. Mori N, Tsugane MH, Yamashita K, Ikuta Y, Yasuda M: Pathogenesis of retinoic acid induced abnormal pad patterns on mouse volar skin. Teratology 2000, 62:181–188
64. Sharov AA, Weiner L, Sharova TY, Siebenhaar F, Atoyan R, Reginato AM, McNamara CA, Funa K, Gilchrest BA, Brissette JL, Botchkarev VA: Noggin overexpression inhibits eyelid opening by altering epidermal apoptosis and differentiation. EMBO J 2003, 22:2992–3003
65. Murakami R, Mizuno T: Proximal-distal sequence of development of the skeletal tissues in the penis of rat and the inductive effect of epithelium. J Embryol Exp Morphol 1986, 92:133–143
66. Hildebrand M: Reproductive system and urogenital ducts. Analysis of Vertebrate Structure, ed 4. New York, John Wiley & Sons, Inc., 1995, pp 299–315
67. Kurzrock EA, Baskin LS, Li Y, Cunha GR: Epithelial-mesenchymal interactions in development of the mouse fetal genital tubercle. Cell Tissue Organ 1999, 164:125–130
68. Yamaguchi TP, A Bradley, AP McMahon, Jones S: A Wnt5a pathway underlies outgrowth of multiple structures in the vertebrate embryo. Development 1999, 126:1211–1223

69. Haraguchi R, Suzuki K, Murakami R, Sakai M, Kamikawa M, Kengaku M, Sekine K, Kawano H, Kato S, Ueno N, Yamada G: Molecular analysis of external genitalia formation: the role of fibroblast growth factor (Fgf) genes during genital tubercle formation. Development 2000, 127:2471–2479
70. Haraguchi R, Mo R, Hui C, Motoyama J, Makino S, Shiroishi T, Gaffield W, Yamada G: Unique functions of Sonic hedgehog signaling during external genitalia development. Development 2001, 128: 4241–4250
71. Murakami R: A histological study of the development of the penis of wild-type and androgen-insensitive mice. J Anat 1987, 153:223–231
72. Hogan BL: Bone morphogenetic proteins in development. Curr Opin Genet Dev 1996, 6:432–438
73. Brown DJ, Kim TB, Petty EM, Downs CA, Martin DM, Strouse PJ, Moroi SE, Milunsky JM, Lesperance MM: Autosomal dominant stapes ankylosis with broad thumbs and toes, hyperopia, and skeletal anomalies is caused by heterozygous nonsense and frameshift mutations in NOG, the gene encoding Noggin. Am J Hum Genet 2002, 71: 618–624
74. Brown DJ, Kim TB, Petty EM, Downs CA, Martin DM, Strouse PJ, Moroi SE, Gebarski SS, Lesperance MM: Characterization of a Stapes Ankylosis Family with a NOG Mutation. Otol Neurotol 2003, 24: 210–215
75. Valenzuela DM, Economides AN, Rojas E, Lamb TM, Nunez L, Jones P, Lp NY, Espinosa III R, Brannan CI, Gilbert DJ: Identification of mammalian Noggin and its expression in the adult nervous system. J Neurosci 1995, 15:6077–6084
76. Bridge J, Sanger W, Mosher G, Buehler B, Hearty C, Olney A, Fordyce R: Partial duplication of distal 17q. Am J Med Genet 1985, 22:229–235
77. Sarri C, Gyftodimou J, Avramopoulos D, Grigoriadou M, Pedersen W, Pandelia E, Pangalos C, Abazis D, Kitsos G, Vassilopoulos D, Brondum-Nielsen K, Petersen MB: Partial trisomy 17q22-qter and partial monosomy Xq27-qter in a girl with a de novo unbalanced translocation due to a postzygotic error: case report and review of the literature on partial trisomy 17qter. Am J Med Genet 1997, 70:87–94
78. Schlichting CD: Phenotypic plasticity. Encyclopedia of Evolution. Edited by M Pagel. Oxford, Oxford University Press, 2002, pp 883–886
79. West PM, Packer C: Sexual selection, temperature, and the lion's mane. Science 2002, 297:1339–1343
80. Grant PR, Grant BR: Unpredictable evolution in a 30-year study of Darwin's finches. Science 2002, 296:707–711
81. Widelitz RB, Jiang TX, Yu M, Shen T, Shen JY, Wu P, Yu Z, Chuong CM: Molecular biology of feather morphogenesis: a testable model for evo-devo research. J Exp Zool, Part B, Mol Dev Evol 2003, 298:109–122